



Cite this: *Dalton Trans.*, 2015, **44**, 20330

Received 29th September 2015,

Accepted 9th November 2015

DOI: 10.1039/c5dt03797b

www.rsc.org/dalton

Two Rh^{III}-substituted polyoxoniobates and their base-induced transformation: [H₂RhNb₉O₂₈]^{6−} and [Rh₂(OH)₄Nb₁₀O₃₀]^{8−†}

Jung-Ho Son^{*a} and Willam H. Casey^{a,b}

Two new rhodium-substituted polyoxoniobates, [H₂RhNb₉O₂₈]^{6−} (RhNb₉) and [Rh₂(OH)₄Nb₁₀O₃₀]^{8−} (Rh₂Nb₁₀) are reported. The two distinct Rh^{III}-substituted niobate clusters behave differently when the pH is raised with TMAOH: the Rh₂Nb₁₀ is stable until pH ~ 12.7, but RhNb₉ dissociates to form RhNb₅ and RhNb₁₀, similar to some of our other metal-substituted niobates, such as the MNb₉ ions (M = Cr or Mn), which transform to MNb₁₀ when the solution pH is raised.

Transition-metal (TM) – substituted polyoxometalates are an important class of materials. The TM-substitution can add catalytic function to the cluster and the polyoxometalate framework adds great redox properties, especially for polyoxomolybdates and -tungstates.¹ In the polyoxoniobate system, a series of TM-substituted decaniobate-type [MNb₉O₂₈]^{x−} (MNb₉, M = Cr–Ni) have been synthesized recently² and add to the Ti-, V- and Cu-substituted polyoxoniobates that were previously known.³ In these studies, the substitution is limited to the early transition metals. For the heavier transition metals, there have been structures reported for Re(CO)₃-, CpRh- or Pt-coordinated (capped) hexaniobates (Nb₆).⁴ However, substitution of 2nd- or 3rd-row transition metals in the polyoxoniobates as atoms internal to the structure, rather than as capping atoms, has not yet been reported to our knowledge, although among the group V polyoxometalates, [H₂Pt^{IV}V₉O₂₈]^{5−} is known in the polyoxovanadate system.⁵

Here we report the synthesis, structure, characterization and photocatalytic H₂ evolution study of two Rh^{III}-substituted niobates. The two compounds reported here have the stoichiometry: [H₂RhNb₉O₂₈]^{6−} (RhNb₉) and [Rh₂(OH)₄Nb₁₀O₃₀]^{8−} (Rh₂Nb₁₀) as tetramethylammonium (TMA) salts (Fig. 1). The structures of these clusters resemble those of two

Cr^{III}-substituted niobates, [H₂CrNb₉O₂₈]^{6−} (CrNb₉) and [Cr₂(OH)₄Nb₁₂O₃₀]^{8−} (Cr₂Nb₁₀) that we previously described.^{2,6}

Substitution of Rh^{III} in the polyoxoniobate structure was challenging. Our previous methods employed for MNb₉ (M = Cr–Ni) generally showed low yield for rhodium substitution (less than 1%).² The low yield might be a result from the notoriously slow reaction rate of ligand substitutions at the Rh^{III} center.⁷ When we attempted to circumvent the slow kinetics with temperature, we found that some Rh^{III} was reduced to Rh⁰ as a gray or black powder mixed with the crude product at the hydrothermal reaction conditions when the temperature was higher than 120 °C. In order to solve this problem, we added hydrogen peroxide in the reaction mixture to prevent reduction of Rh^{III}. Correspondingly the yields were improved when H₂O₂ was added (40% and 7% for Rh₂Nb₁₀ and RhNb₉, respectively). Hydrogen peroxide also might have helped to dissociate the rather stable Nb₆ or Nb₁₀ ions and facilitate the formation of Rh^{III}-substituted structures.⁸

The solution after hydrothermal reaction was typically a mixture of Nb₁₀, Nb₆, RhNb₉ and Rh₂Nb₁₀ ions, as found by electrospray-ionization mass spectra (ESI-MS). We took advantage of the slightly different solubility of each compound to facilitate separation and purification of the Rh-substituted

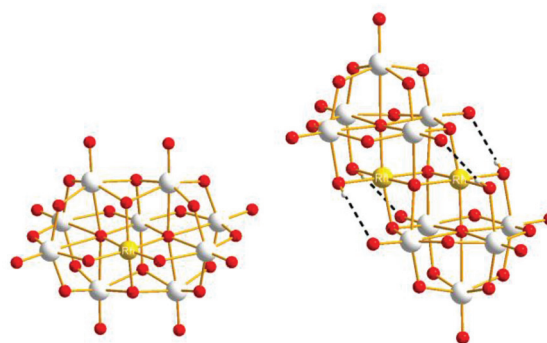


Fig. 1 Ball-and-stick model of RhNb₉ (left) and Rh₂Nb₁₀ (right) (Nb: gray, Rh: gold, O: red). Intramolecular hydrogen bonds are shown with dashed line in Rh₂Nb₁₀.

^aDepartment of Chemistry, University of California, Davis, One Shields Ave. Davis, CA 95616, USA. E-mail: junghoson@gmail.com

^bDepartment of Chemistry, Department of Earth and Planetary Sciences, University of California, Davis, One Shields Ave. Davis, CA 95616, USA

[†]Electronic supplementary information (ESI) available: Experimental details, ESI-MS, FT-IR, UV-Vis data. CCDC 1417431 and 1417432. For ESI and crystallographic data in CIF or other electronic format see DOI: 10.1039/c5dt03797b

molecules. After washing with isopropanol, the product was extracted with ethanol. The ethanol extract was a mixture of $\text{Rh}_2\text{Nb}_{10}$ and Nb_6 ions, and the precipitate that remained after ethanol extraction was a mixture of Nb_{10} and RhNb_9 . The RhNb_9 was separated from Nb_{10} by extraction with ethanol/methanol mixture. Mild heating of the ethanol extract for a few hours caused condensation of more soluble Nb_6 into less soluble Nb_{10} precipitate. The ethanolic orange solution that remained after this heating step consisted of mostly $\text{Rh}_2\text{Nb}_{10}$. The crystalline products of $\text{Rh}_2\text{Nb}_{10}$ and RhNb_9 were obtained after solvent evaporation.

In the crystal structure of RhNb_9 , Rh^{III} is substituted at the central metal site so that it does not possess a terminal oxo group, as we also observed in the $\text{MNb}_9\text{O}_{28}$ ($\text{M} = \text{Cr-Ni}$) series.² The Rh^{III} metal is disordered among the two central sites due to the centrosymmetry, and the sum of Rh^{III} occupancy in those two sites is 1.12, which agrees with stoichiometry of RhNb_9 . Bond valence sum (BVS) calculation of the Rh site is (3.03), indicating the oxidation state of Rh^{III} . The BVS values of two $\text{Rh}-\mu_2\text{-O}-\text{Nb}$ (1.37 and 1.38) are much lower than other bridging oxygen atoms, which suggest that those are protonated, similarly to the substituted MNb_9 ($\text{M} = \text{Cr-Ni}$).² The structure of $\text{Rh}_2\text{Nb}_{10}$ is similar to $\text{Cr}_2\text{Nb}_{10}$, and it can be described as two RhNb_5 Lindqvist-type clusters fused by two $\mu_4\text{-O}$ atoms linking two Rh^{III} and two $\mu_3\text{-O}$ atoms linking Rh^{III} and Nb^{V} . The oxidation state of rhodium in $\text{Rh}_2\text{Nb}_{10}$ is also Rh^{III} , as determined by BVS calculation (2.95). The $\text{Rh}-\text{O}$ bond lengths in $\text{Rh}_2\text{Nb}_{10}$ are longer and more regular (2.0245(16)–2.0605(16) Å) than $\text{Cr}-\text{O}$ bonds in $\text{Cr}_2\text{Nb}_{10}$ (1.9428(13)–2.0131(12) Å). In the structure of $\text{Rh}_2\text{Nb}_{10}$, four protons are found on the four $\text{Rh}-\mu_2\text{-O}-\text{Nb}$, like in the structure of $\text{Cr}_2\text{Nb}_{10}$.⁶ Those protons form intramolecular hydrogen bonds to the neighbouring $\text{Nb}=\text{O}$ ($\text{H}\cdots\text{O}$ distances of 2.309 and 2.386 Å). The ESI-MS spectra of the RhNb_9 and $\text{Rh}_2\text{Nb}_{10}$ agree with their assigned stoichiometries (Fig. S1†).

The pH-dependent stability of the Rh^{III} -substituted niobate clusters was studied by using ESI-MS. When titrated with TMAOH, the golden yellow color of $\text{Rh}_2\text{Nb}_{10}$ solution did not change until highly basic conditions ($\text{pH} \sim 12.9$, Fig. S2†), and most of the $\text{Rh}_2\text{Nb}_{10}$ clusters remained intact for months at this strongly basic condition, as checked by ESI-MS (Fig. S3†). When the solution of RhNb_9 was titrated with TMAOH to this condition, the solution color slowly changed from orange to faint yellow overnight (Fig. S2†). The ESI-MS spectra of the solution after one day (Fig. 2) indicated dissociation of RhNb_9 to RhNb_5 and Nb_6 . Also, formation of a new RhNb_{10} was detectable *via* ESI-MS, which could have formed by self-assembly of dissociated fragments (Fig. 2). It is most likely that this RhNb_{10} would have a similar structure of previously reported $[\text{H}_2\text{Mn}^{\text{IV}}\text{Nb}_{10}\text{O}_{32}]^{8-}$ (MnNb_{10}), in view of their similar ESI-MS pattern.⁹ This observation spurred us to further investigate other TM-substituted polyoxoniobate clusters. We added 50 mg of TMAOH·5H₂O to each aqueous solution containing 30 mg of MNb_9 ($\text{M} = \text{Ti, Cr-Ni}$) and $\text{Cr}_2\text{Nb}_{10}$ clusters to make $\text{pH} \sim 12.6$ and monitored the solution by using ESI-MS (Fig. S4–S10†). The $\text{Cr}_2\text{Nb}_{10}$ clusters were stable at this pH for

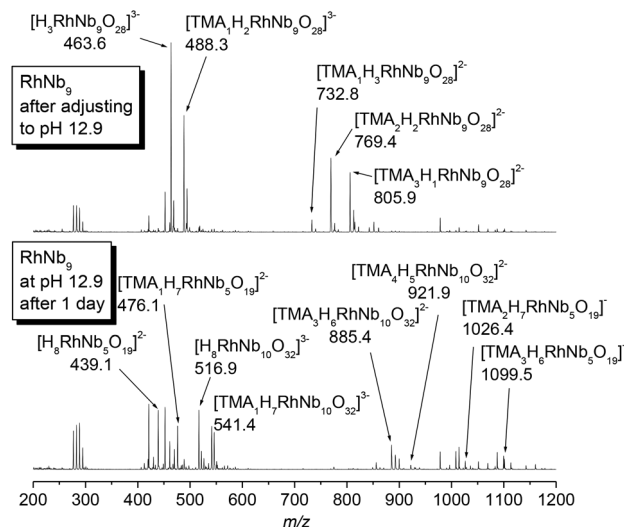
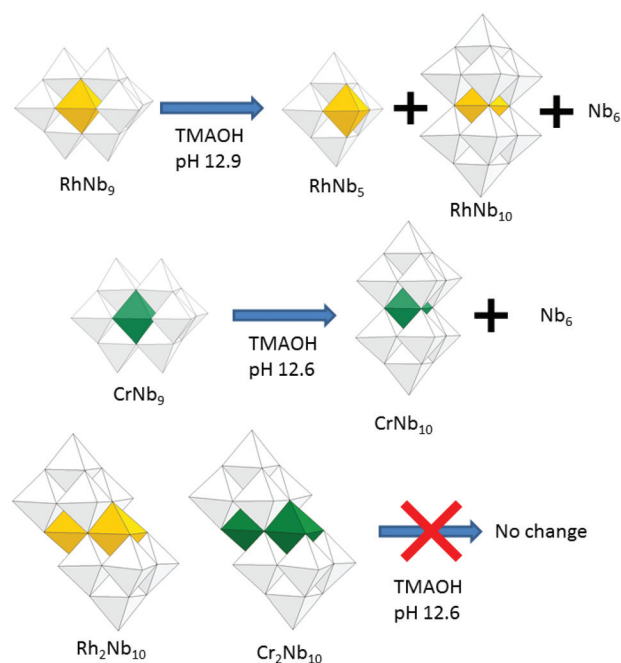


Fig. 2 Change of ESI-MS spectra of RhNb_9 when the solution pH was adjusted to 12.9.

a long period of time, like $\text{Rh}_2\text{Nb}_{10}$ (Fig. S4†). The TiNb_9 , CrNb_9 and MnNb_9 clusters changed in a few days at this high-pH condition. Some Ti_2Nb_8 clusters,^{3a,c,d} formed after a week when the pH of TiNb_9 was increased (Fig. S5†). Considerable amount of CrNb_{10} formed after a few days from the CrNb_9 solution at high pH (Fig. S6†). This result shows that Cr^{III} - and Rh^{III} -substituted polyoxoniobates are not only structurally similar, but also transform *via* similar pathways at high pH (Scheme 1). The color of MnNb_9 solution changed from purple



Scheme 1 Base-induced transformation of MNb_9 and M_2Nb_{10} ($\text{M} = \text{Rh, Cr}$).

to brown with time, suggesting oxidation of Mn^{III} , and ESI-MS spectra after 19 days showed formation of small amount of $\text{Mn}^{\text{IV}}\text{Nb}_{10}$ (Fig. S7†). However, species such as MnNb_5 or CrNb_5 was not detectable, which suggests that they are unstable. Other MNb_9 clusters ($\text{M}=\text{Fe-Ni}$) were relatively stable at the high pH, but small amount of Nb_6 as a decomposition product was detected (Fig. S8–S10†). Thus M_2Nb_{10} ($\text{M}=\text{Rh}^{\text{III}}$ or Cr^{III}) seems to be more stable than MNb_9 at high pH. This higher stability of M_2Nb_{10} is partly attributable to the existence of intramolecular hydrogen bonds, which hold the structure together, perhaps making it less susceptible to base hydrolysis.

When titrated with acid, $\text{Rh}_2\text{Nb}_{10}$ was evident in the ESI-MS spectra until pH 4.0, and RhNb_9 was stable until pH 4.5 (Fig. S11 and S12†), although we recognize that the kinetics of dissociation may be suppressed by inclusion of the Rh^{III} . Both solutions formed hydrous niobium-oxide precipitate below those pH values, which could form without dissociating the structures. On the other hand, we note that the stability window of $\text{Rh}_2\text{Nb}_{10}$ ($4 < \text{pH} < 13$) is similar to $\text{Cr}_2\text{Nb}_{10}$.⁶ The RhNb_9 exhibited a wider stability range ($4.5 < \text{pH} < 12$) than other MNb_9 clusters ($\text{M}=\text{Cr-Ni}$) in general.

The UV-Vis spectra of RhNb_9 and $\text{Rh}_2\text{Nb}_{10}$ are shown in Fig. 3. The $\text{Rh}_2\text{Nb}_{10}$ shows about twice the absorption of visible light relative to the RhNb_9 ion, as expected from the stoichiometry of the clusters. The absorption band of $\text{Rh}_2\text{Nb}_{10}$ (440 nm) is more blue shifted compared to that of RhNb_9 (475 nm), which is responsible for the slightly different colors of the solutions of $\text{Rh}_2\text{Nb}_{10}$ (golden yellow) and RhNb_9 (orange-red). These absorption bands correspond to $^1\text{A}_{1g}$ to $^1\text{T}_{1g}$ or $^1\text{T}_{2g}$ transition of Rh^{III} .¹⁰ The RhNb_9 and $\text{Rh}_2\text{Nb}_{10}$ clusters were also characterized by using FT-IR (Fig. S13†). The FT-IR spectrum of $\text{Rh}_2\text{Nb}_{10}$ show similar feature to that of $\text{Cr}_2\text{Nb}_{10}$ and that of RhNb_9 is similar to those of MNb_9 , which reflect their structural similarity.

TM-substituted polyoxometalates, including polyoxoniobates, have recently been actively studied for use in the water-splitting reaction to generate H_2 and/or O_2 for energy applications.¹¹ We studied H_2 evolution from RhNb_9 and $\text{Rh}_2\text{Nb}_{10}$

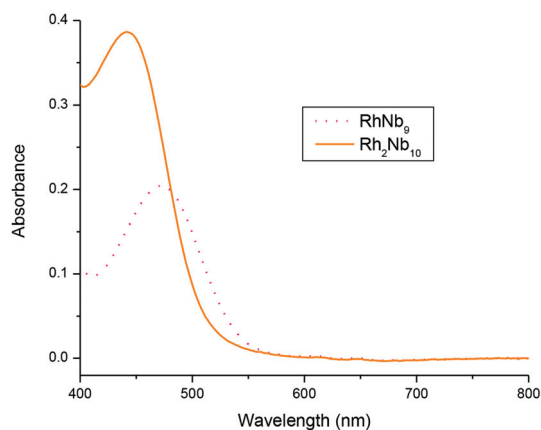


Fig. 3 UV-Vis spectra of 2 mM solution of $\text{Rh}_2\text{Nb}_{10}$ and RhNb_9 without background electrolyte.

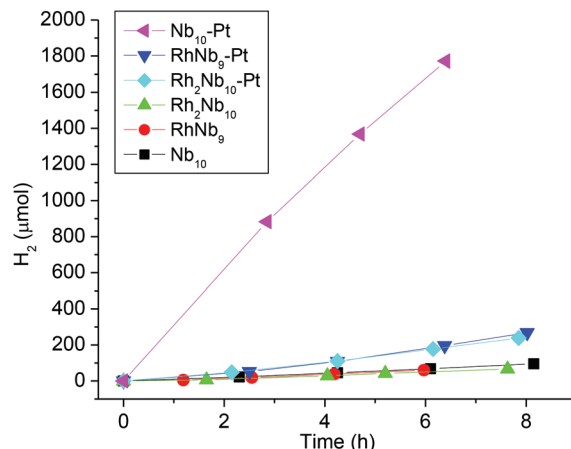


Fig. 4 Comparison of H_2 -evolution activity from the methanol/water solutions (20% v/v) of RhNb_9 , $\text{Rh}_2\text{Nb}_{10}$ and Nb_{10} , with and without H_2PtCl_6 .

ions as a continuation of our previous H_2 -evolution study of the MNb_9 ions ($\text{M}=\text{Cr-Ni}$). When irradiated with visible light, similarly to the MNb_9 ions, neither RhNb_9 nor $\text{Rh}_2\text{Nb}_{10}$ solutions (20% v/v methanol/water) evolved H_2 . Methanol was used as a sacrificial oxidant. The solution did not evolve H_2 without methanol. When a full spectrum from Xe lamp (without UV filter) was employed, however, H_2 evolution was observed ($50 \mu\text{mol g}^{-1} \text{ h}^{-1}$ and $43 \mu\text{mol g}^{-1} \text{ h}^{-1}$, for RhNb_9 and $\text{Rh}_2\text{Nb}_{10}$, Fig. 4). After irradiation, the originally orange-red or yellow solution of RhNb_9 and $\text{Rh}_2\text{Nb}_{10}$ turned greenish brown with small amount of colloids, which probably indicate partial reduction of Rh^{III} to Rh^0 . We have found such colloids in our previous work and are not surprised by them.² The Rh^{II} is known to exhibit a green color.¹⁰ We do not know the amount of Rh^{III} that has been reduced, but comparison of the peak intensities in ESI-MS spectra of the solution before and after irradiation indicated that most of the clusters remained intact (Fig. S14 and S15†). The UV-Vis spectra of $\text{Rh}_2\text{Nb}_{10}$ before and after the irradiation also did not change considerably, but absorption of RhNb_9 solution increased after irradiation, undoubtedly due to the presence of the colloids mentioned above (Fig. S16 and S17†). In the previous H_2 evolution study of the MNb_9 ions ($\text{M}=\text{Cr-Ni}$),² we found that a significant amount of MNb_9 decomposed into Nb_6 and Nb_{10} , with corresponding changes in the UV-Vis spectrum due to the colloid formation. Among them, formation of colloids from NiNb_9 and CoNb_9 positively affected H_2 evolution, while colloid formation from other MNb_9 ($\text{M}=\text{Cr-Fe}$) did not increase the amount of H_2 evolution. In our previous work we have found that the colloids were mixed TM-niobium oxide and they were amorphous, as determined by XRD, TEM and EDX. The relative lack of Nb_6 and Nb_{10} decomposition products after irradiation in the present RhNb_9 and $\text{Rh}_2\text{Nb}_{10}$ suggests that these rhodium RhNb_9 and $\text{Rh}_2\text{Nb}_{10}$ clusters are more stable, perhaps only kinetically so, under the irradiation of intense light when compared to MNb_9 ($\text{M}=\text{Cr-Ni}$). We also compared

H₂-evolution activity of the clusters when H₂PtCl₆ was added as a cocatalyst. In the existence of Pt, Nb₁₀ solution showed ~20 fold increase in the H₂ evolution (1385 μmol g⁻¹ h⁻¹) and amount of precipitate was negligible, but H₂ evolution from RhNb₉ and Rh₂Nb₁₀ after adding H₂PtCl₆ showed only about 3 fold increases (167 and 152 μmol g⁻¹ h⁻¹, respectively) and conspicuous gray-black precipitate formed in the solution (Fig. 4). This presumed Pt–Rh–NbOx precipitate must be responsible for the slight increase of the H₂ evolution, but we did not attempt to characterize it further. The different precipitation behavior of Nb₁₀ and RhNb₉/Rh₂Nb₁₀ after photocatalytic reaction might be due to their different stabilities upon addition of acidic H₂PtCl₆. And the lower H₂ evolution activity of RhNb₉/Rh₂Nb₁₀ compared to Nb₁₀ is likely due to the reduced amount of dissolved clusters in solution caused by precipitation, as seen in ESI-MS (Fig. S14 and S15†).

Conclusions

Two types of new rhodium-substituted polyoxoniobates were synthesized and isolated. The evidences of base-promoted transformation of RhNb₉ to RhNb₅ and RhNb₁₀ suggest a new synthetic strategy for new polyoxoniobates. Such a reaction can be a useful post-synthetic pathway for new polyoxoniobates, instead of commonly employed hydrothermal reaction in the polyoxoniobate chemistry. The transformation of MnNb₉ and CrNb₉ at high pH shows that the stabilities of each TM-substituted decaniobate are different, even if they form similar dissociation products at high pH. The Rh^{III}-substituted polyoxoniobates discussed here are important because these can serve as feedstock to make even more TM-substituted polyoxoniobates, such as RhNb₅ which might have terminal Rh–OH groups.

We thank Jiarui Wang and Prof. Frank E. Osterloh for H₂ evolution measurement. This work was supported by an NSF CCI grant through the Center for Sustainable Materials Chemistry, number CHE-1102637.

Notes and references

- (a) L. C. W. Baker, V. S. Baker, K. Eriks, M. T. Pope, M. Shibata, O. W. Rollins, J. H. Fang and L. L. Koh, *J. Am. Chem. Soc.*, 1966, **88**, 2329; (b) L. C. W. Baker and J. S. Figgis, *J. Am. Chem. Soc.*, 1970, **92**, 3794–3797; (c) T. J. R. Weakley, *J. Chem. Soc., Dalton Trans.*, 1973, 341–346; (d) C. L. Hill and R. B. Brown Jr., *J. Am. Chem. Soc.*, 1986, **108**, 536–538; (e) M. Faraj and C. L. Hill, *J. Chem. Soc., Chem. Commun.*, 1987, 1487–1489; (f) J. Hu and R. C. Burns, *J. Mol. Catal. A: Chem.*, 2002, **184**, 451–464; (g) J.-H. Choi, J. K. Kim, D. R. Park, T. H. Kang, J. H. Song and I. K. Song, *J. Mol. Catal. A: Chem.*, 2013, **371**, 111–117.
- (a) J.-H. Son, J. Wang and W. H. Casey, *Dalton Trans.*, 2014, **43**, 17928–17933; (b) J.-H. Son, C. A. Ohlin and W. H. Casey, *Dalton Trans.*, 2013, **42**, 7529–7533.
- (a) M. Nyman, L. J. Criscenti, F. Bonhomme, M. A. Rodriguez and R. T. Cygan, *J. Solid State Chem.*, 2003, **176**, 111–119; (b) C. A. Ohlin, E. M. Villa, J. C. Fetting and W. H. Casey, *Dalton Trans.*, 2009, 2677–2678; (c) E. M. Villa, C. A. Ohlin, J. R. Rustad and W. H. Casey, *J. Am. Chem. Soc.*, 2009, **131**(45), 16488–16492; (d) E. M. Villa, C. A. Ohlin and W. H. Casey, *J. Am. Chem. Soc.*, 2010, **132**(4), 5264–5272; (e) G. Guo, Y. Xu, J. Cao and C. Hu, *Chem. Commun.*, 2011, **47**, 9411–9413; (f) P. Huang, C. Qin, X.-L. Wang, C.-Y. Sun, G.-S. Yang, K.-Z. Shao, Y.-Q. Jiao, K. Zhou and Z.-M. Su, *Chem. Commun.*, 2012, **48**, 103–105; (g) J.-H. Son, C. A. Ohlin, E. C. Larson, P. Yu and W. H. Casey, *Eur. J. Inorg. Chem.*, 2013, 1748–1753; (h) Y.-T. Zhang, P. Huang, C. Qin, L.-K. Yan, B.-Q. Song, Z.-X. Yang, K.-Z. Shao and Z.-M. Su, *Dalton Trans.*, 2014, **43**, 9847–9850; (i) P. Huang, E.-L. Zhou, X.-L. Wang, C.-Y. Sun, H.-N. Wang, Y. Xing, K.-Z. Shao and Z.-M. Su, *CrystEngComm*, 2014, **16**, 9582–9585; (j) J.-Y. Niu, G. Chen, J.-W. Zhao, P.-T. Ma, S.-Z. Li, J.-P. Wang, M.-X. Li, Y. Bai and B.-S. Ji, *Chem. – Eur. J.*, 2010, **16**, 7082–7086.
- (a) A. V. Besserguenev, M. H. Dickman and M. T. Pope, *Inorg. Chem.*, 2001, **40**(11), 2582–2586; (b) P. A. Abramov, M. N. Sokolov, A. V. Virovets, S. Floquet, M. Haouas, F. Taulelle, E. Cadot, C. Vicent and V. P. Fedin, *Dalton Trans.*, 2015, **44**(5), 2234–2239; (c) P. A. Abramov, C. Vicent, N. B. Kompankov, A. L. Gushchin and M. N. Sokolov, *Chem. Commun.*, 2015, **51**, 4021–4023.
- U. Lee, H.-C. Joo, K.-M. Park, S. S. Mal, U. Kortz, B. Keita and L. Nadjo, *Angew. Chem., Int. Ed.*, 2008, **47**, 793–796.
- J.-H. Son, C. A. Ohlin and W. H. Casey, *Dalton Trans.*, 2012, **41**, 12674–12677.
- (a) J. S. Loring, J. Rosenqvist and W. H. Casey, *J. Colloid Interface Sci.*, 2004, **274**(1), 142–149; (b) J. R. Houston, P. Yu and W. H. Casey, *Inorg. Chem.*, 2005, **44**(14), 5176–5182.
- C. A. Ohlin, E. M. Villa, J. Fetting and W. H. Casey, *Angew. Chem., Int. Ed.*, 2008, **47**, 8251–8254.
- J.-H. Son and W. H. Casey, *Dalton Trans.*, 2013, **42**, 13339–13342.
- F. A. Cotton, G. Wilkinson, C. A. Murillo and M. Bochmann, *Advanced Inorganic Chemistry*, Wiley-Interscience, New York, 6th edn, 1999.
- (a) Z. Zhang, Q. Lin, D. Kurunthu, T. Wu, F. Zuo, S.-T. Zheng, C. J. Bardeen, X. Bu and P. Feng, *J. Am. Chem. Soc.*, 2011, **133**, 6934–6937; (b) P. Huang, C. Qin, Z.-M. Su, Y. Xing, X.-L. Wang, K.-Z. Shao, Y.-Q. Lan and E.-B. Wang, *J. Am. Chem. Soc.*, 2012, **134**, 14004–14010; (c) Z.-L. Wang, H.-Q. Tan, W.-L. Chen, Y.-G. Li and E.-B. Wang, *Dalton Trans.*, 2012, **41**, 9882–9884; (d) J.-H. Son, J. Wang, F. E. Osterloh, P. Yu and W. H. Casey, *Chem. Commun.*, 2014, **50**, 836–838; (e) H. Lv, J. Song, H. Zhu, Y. V. Geletii, J. Bacsá, C. Zhao, T. Lian, D. G. Musaev and C. L. Hill, *J. Catal.*, 2013, **307**, 48–54; (f) H. Lv, W. Guo, K. Wu, Y. V. Geletii, Z. Chen, S. M. Lauinger, J. Bacsá, D. G. Musaev, T. Lian and C. L. Hill, *J. Am. Chem. Soc.*, 2014, **136**, 14015–14018.

